J Eng Math (2015) 92:45–54
DOI 10.1007/s10665-015-9781-2

Combined effects of fluid inertia forces and non-Newtonian rheology in circular stepped squeeze film disks

Jaw-Ren Lin

Received: 21 May 2014 / Accepted: 2 January 2015 / Published online: 13 March 2015

Abstract Based on the Stokes microcontinuum fluid model together with the averaged inertia principle, the combined effects of fluid inertia forces and non-Newtonian rheology on the squeeze film characteristics between circular stepped disks have been presented in this paper. Comparing with the case of a Newtonian lubricant without inertia forces, the influences of convective inertia forces and non-Newtonian couple stresses provide an increase in values of the load-carrying capacity and the approaching time. The improved performances are more pronounced for stepped squeeze films operating with a larger density parameter and couple stress parameter, and a smaller step height ratio and radius ratio.

Keywords Convective inertia forces · Couple stress fluids · Circular stepped disks · Squeeze films

1 Introduction

Research on squeeze film performances plays an important role in many areas of industrial engineering and applied sciences. To satisfy the requirement of modern machine systems operating under severe conditions, the use of various non-Newtonian complex fluids as lubricants has received great attention. Common lubricants exhibiting non-Newtonian behaviors are the natural lubricating fluids, polymer-thickened oils, and base oils blended with certain types of additives. According to the experimental work of Oliver and Shahidullah [1], a polymer-thickened lubricant can provide higher load capacities between of squeeze film strips compared to the case of a Newtonian lubricant. From the experimental results of Scott and Suntiwattana [2], the use of extreme pressure/anti-wear additives can reduce wear of wet clutching materials. In accordance with the experimental study of Spike [3], a lubricating oil blended with suitable additives can stabilize lubricant behavior in elasto-hydrodynamic lubrication contacts. Since the traditional Newtonian continuum theory is not suitable to describe the flow behavior of these kinds of non-Newtonian complex fluids, a number of microcontinuum theories have been generated by Stokes [4], Eringen [5,6] and Ariman et al. [7,8]. In these generations, the Stokes microcontinuum theory of couple stress fluids [4] shows an elegant theory allowing for the presence of body couples and couple stresses. This theory of couple stress fluids is important for scientific and engineering applications of pumping fluids such as human

J.-R. Lin (✉)
Department of Mechanical Engineering, Taoyuan Innovation Institute of Technology,
No. 414, Sec. 3, Jhongshan E. Rd., Jhongli 320, Taiwan
e-mail: jrlin@tiit.edu.tw

bloods [9], synovial fluids [10], and peristaltic flows [11]. On the basis of the microcontinuum theory of Stokes [4], a number of investigators have applied this couple stress fluid model to study the lubrication performance of squeeze film bearings, such as the pure squeeze film journal bearings by Naduvinamani et al. [12] and Reddy et al. [13], the sphere-plate squeeze films by Lin [14] and Elsharkawy and Al-Fadhalah [15], the parallel-plate squeeze films by Ramanaiah [16] and Bujurke et al. [17], and the squeeze films between stepped plates by Kashinath [18]. According to their results, the presence of non-Newtonian couple stresses provides an increase in the load-carrying capacity and the approaching time compared to the traditional case with a Newtonian lubricant. In addition, further studies have also been presented on circular stepped porous bearings operating under different situations, such as the effects of surface roughness and couple stresses by Naduvinamani and Siddangouda [19], and the combined effects of surface roughness and magnetohydrodynamic couple stresses by Naduvinamani et al. [20]. However, the contributions [12–18] have neglected the effects of fluid inertia forces in the study of squeeze film behaviors. Since the effects of film pressure may become more and more significant when the fluid velocity increases, the fluid inertia force effects should be included in the study of squeeze film motions. So far no attempt has been made to investigate the influences of fluid inertia forces on circular stepped squeeze films with a non-Newtonian couple stress fluid. A further study is therefore of interest.

In this paper, the combined effects of fluid inertia forces and non-Newtonian rheology on the squeeze film characteristics between circular stepped disks are presented on the basis the Stokes microcontinuum theory of couple stress fluid model together with the averaged inertia principle. A pressure gradient equation considering the influences of non-Newtonian couple stresses and fluid inertia forces is obtained by employing the momentum integral method. Comparing with the case of a Newtonian lubricant without inertia forces, the results (including the load-carrying capacity and the approaching time) are presented and discussed through the variation of the density parameter, the couple stress parameter, the step height ratio, and the radius ratio of the circular stepped squeeze film.

2 Pressure gradient equation

Figure 1 describes the squeeze film configuration of circular stepped disks lubricated with an incompressible non-Newtonian couple stress fluid. The upper stepped disk with inner radius R_b and outer radius R_a is approaching the lower one with a squeezing velocity $v_s = -\partial h/\partial t$. It is assumed the thin-film theory of hydrodynamic lubrication of Pinkus and Sternlicht [21] is applicable, but the influences of convective fluid inertia forces arising from the temporal acceleration are included. According to the Stokes microcontinuum theory of couple stress fluid model [4], the equations of momentum and continuity in axially cylindrical coordinates (r, θ, z) can be expressed as

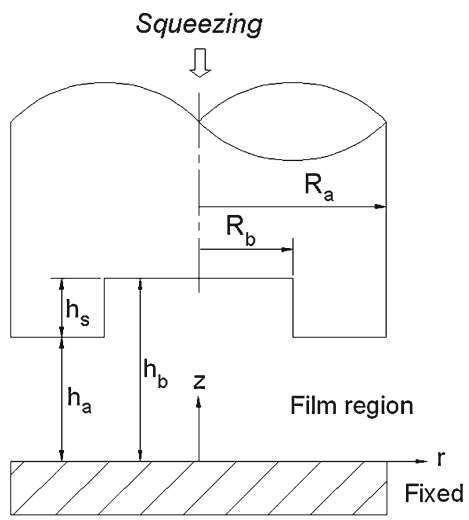

Fig. 1 Squeeze film configuration of circular stepped disks lubricated with a non-Newtonian couple stress fluid

$$\rho\left(u\frac{\partial u}{\partial r}+w\frac{\partial u}{\partial z}\right)=-\frac{\partial p}{\partial r}+\mu\frac{\partial^2 u}{\partial z^2}-\eta\frac{\partial^4 u}{\partial z^4}, \tag{1}$$

$$\frac{\partial p}{\partial z}=0, \tag{2}$$

$$\frac{u}{r}+\frac{\partial u}{\partial r}+\frac{\partial w}{\partial z}=0. \tag{3}$$

In these equations, ρ is the fluid density, p is the fluid pressure, μ is the fluid viscosity, and u and w are the velocity components in the r- and z- directions, respectively. In addition, η represents a new material constant responsible for Stokes couple stress fluids. The relevant boundary conditions for velocity components are the non-slip conditions and the non-couple stress conditions.

$$\text{At}\quad z=0:\quad u=0,\quad \left.\frac{\partial^2 u}{\partial z^2}\right|_{z=0}=0,\qquad w=0. \tag{4}$$

$$\text{At}\quad z=h:\quad u=0\quad \left.\frac{\partial^2 u}{\partial z^2}\right|_{z=h}=0,\qquad w=-v_{\mathrm{s}}. \tag{5}$$

In these equations, the local film height h is

$$h=\begin{cases} h_{\mathrm{b}} & 0\le r\le R_{\mathrm{b}},\\ h_{\mathrm{a}} & R_{\mathrm{b}}\le r\le R_{\mathrm{a}}, \end{cases} \tag{6}$$

where

$$h_{\mathrm{b}}=h_{\mathrm{s}}+h_{\mathrm{a}}, \tag{7}$$

and h_{s} denotes the step height. Since the film height h is small, the convective inertia forces in the momentum can be treated by the averaged inertia principle as proposed by Mahanti and Ramanaiah [22]:

$$\frac{1}{h}\int_0^h \rho\left(u\frac{\partial u}{\partial r}+w\frac{\partial u}{\partial z}\right)\mathrm{d}z=-\frac{\partial p}{\partial r}+\mu\frac{\partial^2 u}{\partial z^2}-\eta\frac{\partial^4 u}{\partial z^4}. \tag{8}$$

Using the relationship of continuity equation and the velocity boundary conditions, the above momentum integral equation can be written as

$$\eta\frac{\partial^4 u}{\partial z^4}-\mu\frac{\partial^2 u}{\partial z^2}=-\frac{\partial p}{\partial r}-\frac{\rho}{h}\left(\frac{\partial}{\partial r}\int_0^h u^2\,\mathrm{d}z+\frac{1}{r}\int_0^h u^2\,\mathrm{d}z\right). \tag{9}$$

To solve for the velocity component, a modified pressure gradient g_{p} is introduced as follows:

$$g_{\mathrm{p}}=\frac{\partial p}{\partial r}+\frac{\rho}{h}\left(\frac{\partial}{\partial r}\int_0^h u^2\,\mathrm{d}z+\frac{1}{r}\int_0^h u^2\,\mathrm{d}z\right). \tag{10}$$

Then one can rewrite the momentum integral equation as

$$\frac{\partial^4 u}{\partial z^4}-\frac{\mu}{\eta}\frac{\partial^2 u}{\partial z^2}=-\frac{1}{\eta}g_{\mathrm{p}}. \tag{11}$$

Employing the boundary conditions for velocity components, the radial velocity component can be obtained from the above differential equation:

$$u = \frac{g_\mathrm{p}}{2\mu}\left\{z^2 - hz + 2l^2\left[1 - \frac{1}{\cosh(h/2l)}\cosh\left(\frac{2z-h}{2l}\right)\right]\right\}, \tag{12}$$

where l is defined as

$$l = \sqrt{\frac{\eta}{\mu}}. \tag{13}$$

In order to derive the pressure gradient equation, the integrals $\int_0^h u\,\mathrm{d}z$ and $\int_0^h u^2\,\mathrm{d}z$ need to be known. Using the expression for the velocity component (12), the integrals give

$$\begin{aligned}\int_0^h u\,\mathrm{d}z &= \frac{g_\mathrm{p}}{2\mu}\int_0^h\left\{z^2 - hz + 2l^2\left[1 - \frac{1}{\cosh(h/2l)}\cosh\left(\frac{2z-h}{2l}\right)\right]\right\}\mathrm{d}z \\ &= \frac{g_\mathrm{p}}{2\mu}\left\{\int_0^h\left(z^2 - hz + 2l^2\right)\mathrm{d}z - \frac{2l^2}{\cosh(h/2l)}\int_0^h\cosh\left(\frac{2z-h}{2l}\right)\mathrm{d}z\right\} = -\frac{g_\mathrm{p}}{12\mu}g_0,\end{aligned} \tag{14}$$

$$\int_0^h u^2\,\mathrm{d}z = \frac{g_\mathrm{p}^2}{4\mu^2}\int_0^h\left\{z^2 - hz + 2l^2\left[1 - \frac{1}{\cosh(h/2l)}\cosh\left(\frac{2z-h}{2l}\right)\right]\right\}^2\mathrm{d}z = \frac{g_\mathrm{p}^2}{4\mu^2}g_1, \tag{15}$$

where the functions g_0 and g_1 are defined by

$$g_0(h,l) = h^3 - 12l^2h + 24l^3\tanh\left(\frac{h}{2l}\right) \tag{16}$$

and

$$g_1(h,l) = \frac{1}{30}h^5 - \frac{2}{3}l^2h^3 + 2l^4h\left[7 - \tanh^2\left(\frac{h}{2l}\right)\right] - 28l^5\tanh\left(\frac{h}{2l}\right). \tag{17}$$

Substituting the result of integral $\int_0^h u^2\,\mathrm{d}z$ into the right-hand side of Eq. (10), one can obtain the expression for pressure gradient function $\partial p/\partial r$ as

$$\frac{\partial p}{\partial r} = g_\mathrm{p} - \frac{1}{4\mu^2}\frac{\rho}{h}\left[\frac{\partial}{\partial r}\left(g_\mathrm{p}^2 g_1\right) + \frac{1}{r}\left(g_\mathrm{p}^2 g_1\right)\right]. \tag{18}$$

For each region $0 \le r \le R_\mathrm{b}$ and $R_\mathrm{b} \le r \le R_\mathrm{a}$, respectively, the film height is independent of the radial coordinate.

On the other hand, the equation for the squeeze motion is

$$\int_0^h u\,\mathrm{d}z = \frac{1}{2}r v_\mathrm{s}. \tag{19}$$

Equating the right-hand side of Eqs. (14) and (19), one can obtain another expression of the modified pressure gradient function:

$$g_p = -\frac{6\mu}{g_0}r v_\mathrm{s}. \tag{20}$$

Substituting this expression for the modified pressure gradient g_p into Eq. (18) and performing the derivative, one can derive the pressure gradient equation for the squeeze film:

$$\frac{\partial p}{\partial r} = -\frac{6\mu}{g_0}r v_\mathrm{s} - \frac{27\rho}{h}\frac{g_1}{g_0^2}r v_\mathrm{s}^2. \tag{21}$$

The above equation can be applied to investigate the circular stepped squeeze film characteristics considering the influences of non-Newtonian couple stresses and convective fluid inertia forces.

3 Squeeze film performance

In order to analyze the squeeze film performance, the following non-dimensional variables and parameters are introduced:

$$r^* = \frac{r}{R_a}, \quad p^* = \frac{p}{p_r}, \quad p_a^* = \frac{p_a}{p_r}, \quad p_b^* = \frac{p_b}{p_r}, \quad h_a^* = \frac{h_a}{h_{a0}}, \quad h_b^* = \frac{h_b}{h_{a0}}, \quad h^* = \frac{h}{h_{a0}}, \tag{22a}$$

$$g_0^* = \frac{g_0}{h_{a0}^3}, \quad g_1^* = \frac{g_1}{h_{a0}^5}, \quad V^* = \frac{6\mu R_a^2 v_s}{p_r h_{a0}^3}, \quad \alpha = \frac{R_b}{R_a}, \quad \beta = \frac{h_s}{h_{a0}}, \quad \varphi = \frac{l}{h_{a0}}, \quad \delta = \frac{\rho h_{a0}^4 p_r}{6\mu^2 R_a^2}, \tag{22b}$$

where p_r is the ambient pressure, h_{a0} is the initial minimum film height, and the superscript "*" represents the non-dimensional quantity of the variables. In addition, α denotes the non-dimensional radius ratio, β is the non-dimensional step height ratio, φ is the non-dimensional couple stress parameter, and δ is the non-dimensional density parameter. Then the pressure gradient equation can be written in a non-dimensional form:

$$\frac{\partial p_b^*}{\partial r^*} = -\left[\frac{1}{g_{0b}^*} V^* + \frac{9\delta g_{1b}^*}{2h_b^* g_{0b}^{*2}} V^{*2}\right] r^*, \qquad 0 \le r^* \le \alpha, \tag{23}$$

$$\frac{\partial p_a^*}{\partial r^*} = -\left[\frac{1}{g_{0a}^*} V^* + \frac{9\delta g_{1a}^*}{2h_a^* g_{0a}^{*2}} V^{*2}\right] r^*, \qquad \alpha \le r^* \le 1 \tag{24}$$

where

$$h^* = \begin{cases} h_b^* & 0 \le r^* \le \alpha, \\ h_a^* & \alpha \le r^* \le 1, \end{cases} \tag{25}$$

$$h_b^* = \beta + h_a^*, \tag{26}$$

$$g_{0b}^* = g_0^*(h_b^*, \varphi), \tag{27}$$

$$g_{0a}^* = g_0^*(h_a^*, \varphi), \tag{28}$$

$$g_0^*(h^*, \varphi) = h^{*3} - 12\varphi^2 h^* + 24\varphi^3 \tanh\left(\frac{h^*}{2\varphi}\right), \tag{29}$$

$$g_1^*(h^*, \varphi) = \frac{1}{30} h^{*5} - \frac{2}{3}\varphi h^{*3} + 2\varphi^4 h^* \left[7 - \tanh^2\left(\frac{h^*}{2\varphi}\right)\right] - 28\varphi^5 \tanh\left(\frac{h^*}{2\varphi}\right). \tag{30}$$

The boundary conditions for the non-dimensional film pressure are $p_a^* = 1$ at $r^* = 1$, and $p_a^* = p_b^*$ at $r^* = \alpha$. Integrating the non-dimensional pressure gradient equation with respect to r^* and applying the pressure boundary conditions, one can derive the non-dimensional film pressure:

$$p_b^* = -\frac{1}{2} r^{*2}\left(\frac{1}{g_{0b}^*} V^* + \frac{9\delta g_{1b}^*}{2h_b^* g_{0b}^{*2}} V^{*2}\right) + c_1, \qquad 0 \le r^* \le \alpha, \tag{31}$$

$$p_a^* = 1 + \frac{1}{2}\left(1 - r^{*2}\right)\left(\frac{1}{g_{0a}^*} V^* + \frac{9\delta g_{1a}^*}{2h_a^* g_{0a}^{*2}} V^{*2}\right), \qquad \alpha \le r^* \le 1, \tag{32}$$

where

$$c_1 = 1 + \frac{1}{2}\left(\frac{1-\alpha^2}{g_{0a}^*} + \frac{\alpha^2}{g_{0b}^*}\right) V^* + \frac{9\delta}{4}\left[\frac{(1-\alpha^2) g_{1a}^*}{h_a^* g_{0a}^{*2}} + \frac{\alpha^2 g_{1b}^*}{h_b^* g_{0b}^{*2}}\right] V^{*2}. \tag{33}$$

The load-carrying capacity W is evaluated by integrating the film pressure field acting on the stepped disk surface:

$$W = 2\pi \int_0^{R_b} (p_b - p_r) r \, dr + 2\pi \int_{R_b}^{R_a} (p_a - p_r) r \, dr. \tag{34}$$

Expressed in a non-dimensional form and using the expression of the film pressure, the non-dimensional load capacity W^* can be derived after integrating the equation:

$$W^* = \frac{8W}{\pi R_a^2 p_r} = W_0^* V^* + W_1^* \delta V^{*2}, \tag{35}$$

where

$$W_0^* = 2\left[\frac{1-\alpha^4}{g_{0a}^*} + \frac{\alpha^4}{g_{0b}^*}\right], \tag{36}$$

$$W_1^* = 9\left[\frac{(1-\alpha^4) g_{1a}^*}{h_a^* g_{0a}^{*2}} + \frac{\alpha^4 g_{1b}^*}{h_b^* g_{0b}^{*2}}\right]. \tag{37}$$

To obtain the approaching time, a non-dimensional definition t^* is introduced:

$$t^* = \frac{h_{a0}^2 p_r}{6\mu R_a^2} t. \tag{38}$$

Then, the non-dimensional squeezing velocity can be expressed as:

$$V^* = \frac{6\mu R_a^2 v_s}{p_r h_{a0}^3} = -\frac{dh_a^*}{dt^*}. \tag{39}$$

Substituting into Eq. (35) results in the differential equation governing the film height varying with the approaching time,

$$\frac{dh_a^*}{dt^*} = \frac{W_0^* - [W_0^{*2} + 4\delta W^* W_1^*]^{1/2}}{2\delta W_1^*}. \tag{40}$$

Applying the initial condition for the non-dimensional film height $h_a^*(t^* = 0) = 1$, the non-dimensional approaching time can be derived by integrating the differential equation:

$$t^* = \int_{h_a^*}^{1} \frac{2\delta W_1^*}{[W_0^{*2} + 4\delta W^* W_1^*]^{1/2} - W_0^*} \, dh_a^*. \tag{41}$$

Using the method of Gaussian quadrature, the numerical values of the approaching time can be evaluated.

4 Results and discussion

According to the above analysis, the geometry of the stepped disk is defined by the radius ratio α and the step height ratio β. In addition, φ is the couple stress parameter dominating the influences of non-Newtonian property, and δ is the density parameter characterizing the effects of fluid inertia forces. For $\delta = 0$, the present study reduces to the case of a non-Newtonian circular stepped squeeze film without fluid inertia forces. For $\delta = 0$ and $\varphi = 0$, the present analysis reduces to the case of a Newtonian circular stepped squeeze film neglecting fluid inertia effects.

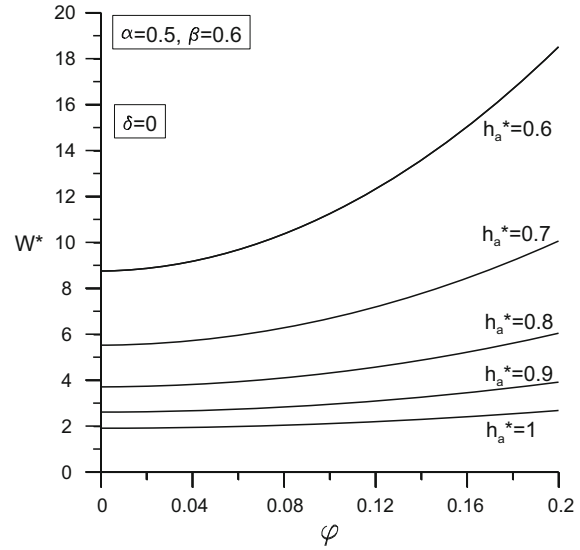

Fig. 2 Load capacity W^* varying with couple stress parameter φ for different h_a^* with $\alpha = 0.5$ and $\beta = 0.6$ under the non-inertia case ($\delta = 0$)

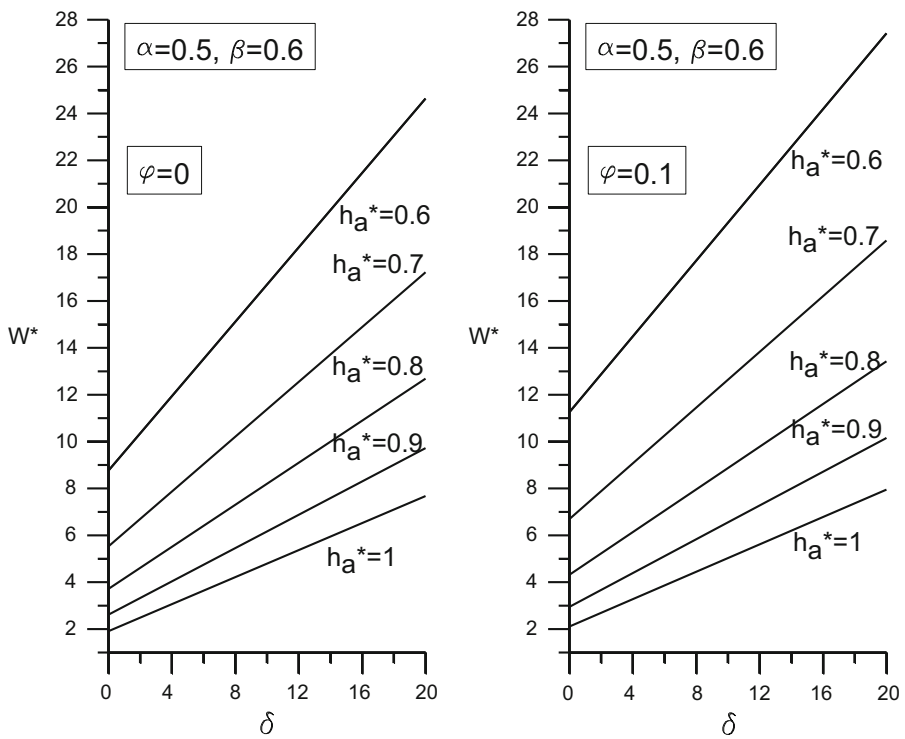

Fig. 3 Load capacity W^* varying with density parameter δ for different h_a^* with $\alpha = 0.5$ and $\beta = 0.6$ under both the Newtonian-lubricant ($\varphi = 0$) and non-Newtonian-lubricant ($\varphi = 0.1$) cases

Figure 2 shows load capacity W^* varying with couple stress parameter φ for different h_a^* with $\alpha = 0.5$ and $\beta = 0.6$ under the non-inertia case ($\delta = 0$). It is observed that the presence of couple stresses ($\varphi \neq 0$) provides an increase in the load-carrying capacity compared to the Newtonian-lubricant case ($\varphi = 0$); and larger increments are obtained with the decreasing value of h_a^* or the increasing value of φ. Figure 3 displays the load capacity W^* varying with density parameter δ for different h_a^* with $\alpha = 0.5$ and $\beta = 0.6$ under both the Newtonian-lubricant ($\varphi = 0$) and non-Newtonian-lubricant ($\varphi = 0.1$) cases. The load capacity is observed to increase with the increasing values

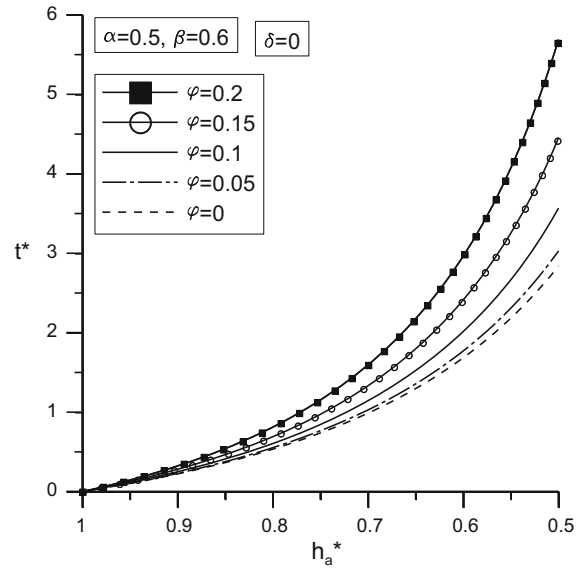

Fig. 4 Approaching time t^* varying with film height h_a^* for different φ with $\alpha = 0.5$ and $\beta = 0.6$ under the non-inertia case ($\delta = 0$)

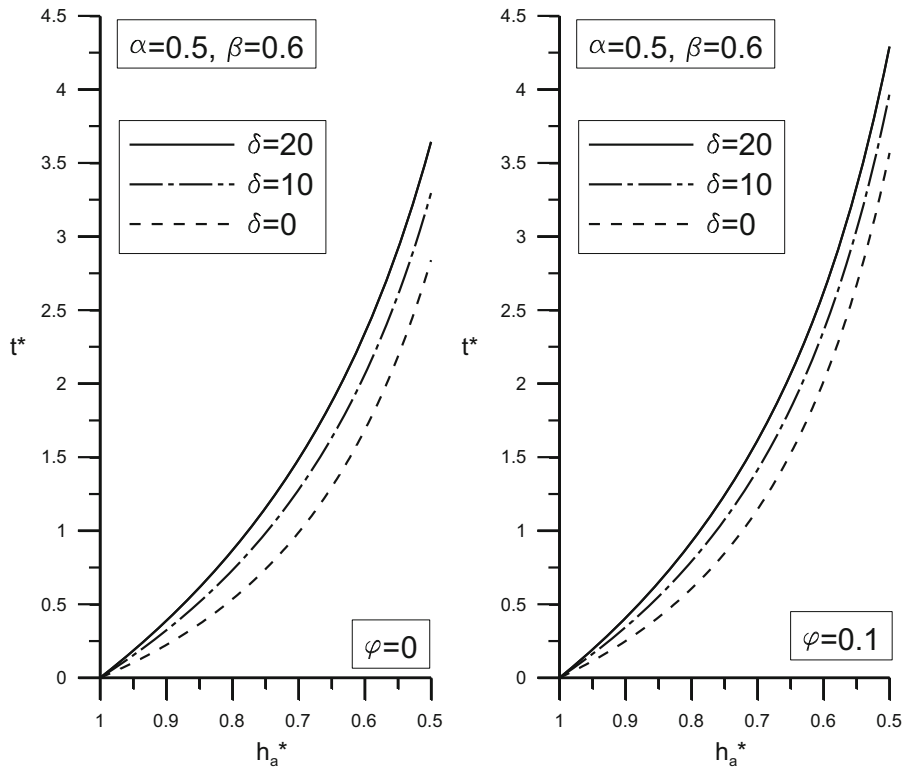

Fig. 5 Approaching time t^* varying with film height h_a^* for different δ with $\alpha = 0.5$ and $\beta = 0.6$ under both the Newtonian-lubricant ($\varphi = 0$) and non-Newtonian-lubricant ($\varphi = 0.1$) cases

of the density parameter. In addition, the combined effects of fluid inertia forces and non-Newtonian couple stresses on the load capacity are more emphasized at a lower film height. Figure 4 describes the approaching time t^* varying with film height h_a^* for different φ with $\alpha = 0.5$ and $\beta = 0.6$ under the non-inertia case ($\delta = 0$). It is seen that the presence of couple stresses results in an increase in the approaching time. These phenomena can be understood

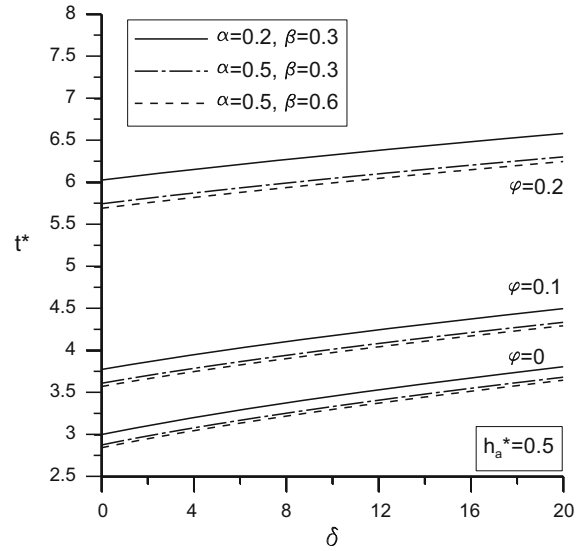

Fig. 6 Approaching time t^* varying with density parameter δ for different α and β with $h_a^* = 0.5$ under both the Newtonian-lubricant ($\varphi = 0$) and non-Newtonian-lubricant ($\varphi = 0.1, 0.2$) cases

that since the effects of non-Newtonian couple stresses provide a higher load-carrying capacity, a higher film height would be achieved for the same time to be taken compared to the case with a Newtonian lubricant. Figure 5 depicts the approaching time t^* varying with film height h_a^* for different δ with $\alpha = 0.5$ and $\beta = 0.6$ under both the Newtonian-lubricant ($\varphi = 0$) and non-Newtonian-lubricant ($\varphi = 0.1$) cases. Since the influences of fluid inertia forces result in a higher load-carrying capacity as described in Fig. 3, a longer approaching time is obtained for the circular stepped squeeze film compared to the non-inertia case. Further increments of the approaching time are predicted for the squeeze film with a non-Newtonian couple stress fluid ($\varphi = 0.1$). Figure 6 shows the approaching time t^* varying with density parameter δ for different α and β with $h_a^* = 0.5$ under both the Newtonian-lubricant ($\varphi = 0$) and non-Newtonian-lubricant ($\varphi = 0.1, 0.2$) cases. For the circular stepped disks with the radius ratio $\alpha = 0.5$ and the step height ratio $\beta = 0.6$ under the Newtonian-lubricant ($\varphi = 0$) case, the approaching time increases with the increasing values of the density parameter. Decreasing the radius ratio and the step height ratio ($\alpha = 0.5, \beta = 0.3; \alpha = 0.3, \beta = 0.3$) increases the increments of the approaching time. When the effects of non-Newtonian couple stresses ($\varphi = 0.1, 0.2$) are included, larger increments of the approaching time are obtained.

The present work is mainly concerned with the combined effects of fluid inertia forces arising from the temporal acceleration and non-Newtonian rheology on the squeeze film characteristics between circular stepped disks. The microcontinuum theory intends to account for particle size influences of fluids involving substructure. The non-Newtonian effects of couple stresses could be regarded as the behavior of one part of a deforming element on its neighbourhood as Stokes [4]. On the whole, the combined effects of convective inertia forces and non-Newtonian couple stresses provide an increase in the load-carrying capacity and a longer approaching time compared to the non-inertia Newtonian-lubricant case, especially for the stepped disks operating with larger values of the density parameter and the couple stress parameter. So far, the results of experimental and theoretical studies are not available. However, a study of the effects of surface roughness and couple stresses on porous circular stepped squeeze films is presented by Naduvinamani and Siddangouda [19]. A pressure gradient equation has been derived in their Eq. (25). Ignoring the effects of surface roughness and porous material, their Eq. (25) using the same notation as the present study reduces to

$$\frac{\partial p}{\partial r} = -\frac{6\mu}{h^3 - 12l^2h + 24l^3 \tanh(h/2l)} r v_s. \tag{42}$$

It agrees well with the present derivation of Eq. (20) when we neglect the inertial force term, $27\rho g_1 r v_s^2/(h g_0^2)$.

5 Conclusions

A pressure gradient equation considering the influences of non-Newtonian couple stresses and fluid inertia forces is obtained on the basis of the Stokes microcontinuum fluid model together with the averaged inertia principle. Comparing with the case of a Newtonian lubricant without inertia forces, the influences of fluid inertia forces and non-Newtonian couple stresses provide increases in the load-carrying capacity and the approaching time. The improved squeeze film performances are more emphasized for circular stepped disks operating with a larger value of the density parameter and the couple stress parameter, and a smaller value of the step height ratio and the radius ratio.

References

1. Oliver DR, Shahidullah M (1983) Load enhancement effects by polymer-thickened oils in strip squeeze film flow. J Non-Newton Fluid Mech 13:93–102
2. Scott W, Suntiwattana P (1995) Effect of oil additives on the performance of a wet friction clutch material. Wear 181–183:850–855
3. Spikes AH (1994) The behavior of lubricants in contacts: current understanding and feature possibilities. J Proc Inst Mech Eng 28:3–15
4. Stokes VK (1966) Couple stresses in fluids. Phys Fluids 9:1709–1715
5. Eringen AC (1964) Simple micropolar fluids. Int J Eng Sci 2:203–217
6. Eringen AC (1966) Theory of micropolar fluids. J Math Mech 16:1–18
7. Ariman T, Turk MA, Sylvester ND (1973) Microocontinuum fluid mechanics-a review. Int J Eng Sci 11:905–930
8. Ariman T, Turk MA, Sylvester ND (1974) Applications of microcontinuum fluid mechanics. Int J Eng Sci 12:273–293
9. Srivastava LM (1985) Flow of couple stress fluid through stenotic blood vessels. J Biomech 18:479–485
10. Bujurke NM, Kudenatti RB (2006) An analysis of rough poroelastic bearings with reference to lubrication mechanism of synovial joints. Appl Math Comput 178:309–320
11. Shehawey EFE, Mekheimer KS (1994) Couple stresses in peristaltic transport of fluids. J Phys D 27:1163–1170
12. Naduvinamani NB, Hiremath PS, Gurubasavaraj G (2001) Squeeze film lubrication of a short porous journal bearing with couple stress fluids. Tribol Int 34:739–747
13. Reddy GJC, Reddy CE, Prasad KRK (2008) Effect of viscosity variation on the squeeze film performance of a narrow hydrodynamic journal bearing operating with couple stress fluids. Proc. IMechE Part J: Journal of Engineering. Tribology 222:141–150
14. Lin JR (2000) Squeeze film characteristics between sphere and a flat plate: couple stress fluid model. Comput Struct 75:73–80
15. Elsharkawy AA, AL-Fadhalah KJ (2008) Separation of a sphere from a flat in the presence of couple stress fluids. Lubr Sci 20:61–74
16. Ramanaiah G (1979) Squeeze films between finite plates lubricated by fluids with couple stresses. Wear 54:315–320
17. Bujurke NM, Salimath CS, Kudenatti RB, Shiralashetti SC (2007) Wavelet-multigrid analysis of squeeze film characteristics of poroelastic bearings. J Comput Appl Math 203:237–248
18. Kashinath B (2012) Squeeze film lubrication between parallel stepped plates with couplestress fluids. Int J Stat Math 3:65–69
19. Naduvinamani NB, Siddangouda A (2007) Combined effects of surface roughness and couple stresses on squeeze film lubrication between porous circular stepped plates. Proc IMechE J 221:525–534
20. Naduvinamani NB, Hanumagowda BN, Fathima ST (2012) Combined effects of MHD and surface roughness on couple-stress squeeze film lubrication between porous circular stepped plates. Tribol Int 56:19–29
21. Pinkus O, Sternlicht B (1961) Theory of hydrodynamic lubrication. McGraw-Hill, New York
22. Mahanti AC, Ramanaiah GR (1976) Inertia effect of micropolar fluid squeeze film bearings and thrust bearings. Wear 39:227–238